Short communication

On the role of bismuth as modifier in AuPdBi catalysts: Effects on liquid-phase oxidation and hydrogenation reactions

Sebastiano Campisi [a,*], Sofia Capelli [a], Michele Ferri [a], Alberto Villa [a], Ellie Dann [b], Austin Wade [c], Peter P. Wells [d,e,f], Nikolaos Dimitratos [g,**]

[a] *Dipartimento di Chimica, Università degli Studi di Milano, via Golgi 19, 20133 Milano, Italy*
[b] *Department of Chemistry, University College London, London, UK*
[c] *Thermo Fisher Scientific, 5350 NW Dawson Creek Drive, Hillsboro, OR, USA*
[d] *School of Chemistry, University of Southampton, Southampton SO17 1BJ, UK*
[e] *UK Catalysis Hub, Research Complex at Harwell, Rutherford Appleton Laboratory, Harwell Oxon, Didcot OX11 0FA, UK*
[f] *Diamond Light Source Ltd., Harwell Science and Innovation Campus, Chilton, Didcot OX11 0DE, UK*
[g] *Dipartimento di Chimica Industriale e dei Materiali, ALMA MATER STUDIORUM Università di Bologna, Viale Risorgimento 4, 40136 Bologna, Italy*

ARTICLE INFO

ABSTRACT

There is much about the action of bismuth within heterogeneous catalysis that still require a deeper understanding. We observed that, when Bi was added to AuPd bimetallic nanoparticles (NPs) supported on activated carbon, Bi affected the activity and significantly alters the selectivity in two model liquid phase reactions, namely the oxidation of cinnamyl alcohol and the hydrogenation of cinnamaldehyde. A combination of transmission electron microscopy and X-ray absorption spectroscopy provided a detailed characterization of trimetallic AuPdBi systems. We propose that the introduction of bismuth on AuPd NPs results in a partial blockage of most active sites, limiting the occurrence of consecutive reactions.

1. Introduction

Being a non-precious and environmentally friendly metal, bismuth has attracted increasing interest as a suitable alternative to replace more expensive, corrosive, and toxic industrial catalysts. Bismuth has been proposed as catalyst for several chemical transformations either in the form of salts or organometallic compounds [1].

Furthermore, similarly to other *p*-electron metals (e.g. Pb, Sn, Sb), when added in low concentration, bismuth has demonstrated to act as promoter and/or modifier of noble metal catalysts [2]. The modification with Bi has been reported to affect the catalytic performances of Pd-, Pt- and Au-based catalysts in several reactions, such as the selective oxidation of biomass derived substrates (e.g. alcohols [2–6], glycerol [7,8], glucose [9], 5-hydroxymethylfurfural [10], glyoxal [11]), the hydrochlorination of acetylene [12], the oxygen reduction reaction (ORR) [13], hydrogenation reactions [14], the electrooxidation of formic acid [15] or NaBH$_4$ [16] for hydrogen production, and many others.

Trimetallic Au-Pd-Bi catalysts have been already demonstrated to

exhibit unique selectivity and stability in alcohol oxidation processes. Although numerous studies appeared investigating the nature of the promoter role of Bi by advanced ex situ and in situ characterization techniques [6,17–20], this subject still remains a matter of debate. Various interpretations have been proposed for the promotional effects; for example including (i) the geometric blocking of low-selectivity sites (edges, corners, terraces) on the noble metal nanoparticles, (ii) modification of the electronic properties of the vicinal noble metal atoms and the subsequent effects on adsorption properties, (iii) the stabilization of metal phases, and (iv) the ligand effects by the formation of complexes among bismuth and noble metal atoms and the adsorbed reactants/products. Further complicating matters, the nature and the role of bismuth strongly depends on the experimental procedure followed for its deposition on the catalyst surface. Depending on the synthesis conditions, different location and speciation of Bi can be obtained, alternatively resulting either in the formation of a trimetallic ensemble or more segregated systems [21,22].

In this work, we have investigated the role of Bi as modifier of

---

bimetallic well-defined Au—Pd nanoparticles supported on carbon, when used as catalysts for oxidation and hydrogenation reactions. Cinnamyl alcohol and cinnamaldehyde were selected as model substrates due to the fact we can study the preferential oxidation of the C-OH, C=O, and preferential reduction of C=C, C=O functional groups.

According to Scheme S1, the cinnamyl alcohol oxidation can proceed through a complex pathway leading to a large variety of products. The dehydrogenation of the hydroxyl group produces cinnamaldehyde, an interesting product with application in food industry as flavoring, in agrochemistry as insecticide and in metallurgy as corrosion inhibitor. Cinnamyl alcohol can also undergo hydrogenolysis resulting in the production of trans-1-phenyl-1-propene or hydrogenation of the carbon–carbon double bond to form 3-phenyl-1-propanol. Both trans-1-phenyl-1-propene and 3-phenyl-1-propanol can be further transformed into 1-phenylpropane, used as solvent in printing ink industry and textile industry.

Although the occurrence of hydrogenolysis and hydrogenation reaction might sound implausible in oxidative conditions, it finds adequate explanation in the reaction mechanism, involving formation of metal-hydride species [23,24]. The latter can then transfer hydrogen to the adsorbed reagent or product molecules. Indeed, also cinnamaldehyde can be hydrogenated to 3-phenylpropanal. In addition, cinnamaldehyde can be decarbonylated to CO and styrene, while carbon-carbon bond cleavage leads to benzaldehyde.

Similarly to cinnamyl alcohol oxidation reaction, the presence of many functional groups in the substrate is responsible for the complex reaction pathway of the cinnamaldehyde hydrogenation reaction (Scheme S2). The hydrogenation of cinnamaldehyde can involve either the alkenyl group or the carbonyl group. In the former case 3-phenylpropanal, a compound widely used as artificial flavoring additive in food and cosmetics, is produced. The selective hydrogenation of carbonyl group leads to cinnamyl alcohol, which can undergo hydrogenolysis to trans-1-phenyl-1-propene. The hydrogenation of both carbonyl and alkenyl group results in the formation of 3-phenyl-1-propanol. Both trans-1-phenyl-1-propene and 3-phenyl-1-propanol can be converted into 1-phenylpropane.

Herein, the comparison between two different Bi deposition experimental procedures as well as the use of a combination of several characterization techniques (transmission electron microscopy, X-rays absorption spectroscopy) help in determining the structure-activity relationships of trimetallic Au-Pd-Bi catalysts with respect to analogue Au—Pd catalysts.

2. Experimental

2.1. Catalyst preparation

2.1.1. Monometallic Pd/AC preparation

Solid Na_2PdCl_4 (0.051 mmol) (Sigma-Aldrich, purity >99.9%) and 1 mL of a PVA solution (1 wt%) were mixed in 0.1 L of H_2O (Pd:PVA 1/0.5 wt/wt%), forming a yellow solution. After 3 min, a precise volume of 0.1 M of $NaBH_4$ solution (Pd/$NaBH_4$ 1/8 mol/mol) was added in the solution under magnetic stirring and a colloid was produced. Within a few minutes of colloid generation the pH was regulated to the value of 2 by addition of sulphuric acid and the support was added to the vigorously stirring colloidal solution. The amount of the support was accurately weighed in order to obtain a final metal loading of 1 wt% (in the assumption of quantitative loading of the metal on the support). The catalysts were filtered and washed several times and dried at 100 °C for 2 h.

2.1.2. Bimetallic AuPd/AC preparation

Solid $NaAuCl_4 \cdot 2H_2O$ (0.062 mmol) and Na_2PdCl_4 (0.040 mmol) (Au/Pd ratio 0.73/0.27 wt%) and 2 mL of a PVA solution (1 wt%) were mixed in 0.2 L of H_2O (Au/PVA 1/0.5 wt/wt%). After 3 min, a 0.1 M of $NaBH_4$ solution (Au/$NaBH_4$ 1/4 mol/mol) was added to the solution

under vigorous magnetic stirring. Within a few minutes of their generation, the colloids (after pH regulation to pH = 2, by sulphuric acid) were immobilized by dispersing the support in the vigorously stirring colloidal solution. The amount of the support was controlled in order to obtain a final metal loading of 1 wt% (on the basis of quantitative loading of the metal on the support). The catalysts were filtered and washed several times and dried at 100 °C for 2 h.

2.1.3. Trimetallic AuPdBi/AC and physical mixture preparation

Bismuth was added to a portion of AuPd/AC prepared with the methodology reported above. $BiO(NO)_3$ (0.12 mmol) was dissolved in 100 mL of distilled water at pH = 2 (pH modified using concentrated H_2SO_4). Bi amount was calculated in order to have a final loading of 1%. AuPd/AC was added to the solution and left under stirring for 2 h. The solid was re-dispersed in 100 mL of distilled water and a 0.1 M fresh solution of $NaBH_4$ (metal/$NaBH_4$ = 1:1 mol/mol) was added under stirring. The catalyst was filtered, thoroughly washed with distilled water and dried at 100 °C for 2 h.

For physical mixture preparation, solid Bi_2O_3 and AuPd/AC were physically mixed before adding to the reactor. The amount of Bi_2O_3 was calculated in order to have the same Bi loading as in the previous catalyst 1%Bi.

2.2. Catalyst characterization

2.2.1. Electron microscopies

STEM/EDX measurements were performed on a FEI Talos 200× scanning transmission electron microscope equipped with a Super-X energy dispersive X-ray spectrometer at the University of Manchester. AuPd/C particles were dry dispersed on lacey-C Cu grids with high-angle annular dark-field (HAADF) imaging and EDS mapping performed with an accelerating voltage of 200 kV. L-family X-rays were used for generation of Au and Pd background subtracted X-ray intensity maps. SEM measurements were performed on a TESCAN MAIA 3 field emission gun scanning electron microscope operating at 15 Kv. EDX maps were acquired on an Oxford Instruments X-MAX^N 80 detector.

2.2.2. X-ray absorption spectroscopy

X-ray absorption spectroscopy measurements were carried out on the B18 beamline, Diamond Light Source, UK. All measurements were carried out in fluorescence mode using a 9-element solid state Ge detector. A Si (111) double crystal monochromator (DCM) was used for measurements of the L-edges of Au and Bi, with a Si (311) DCM was used for the Pd K-edge. Each scan was ~30 min, with a minimum of 3 scans required to achieve an appropriate signal-to-noise ratio. The merged spectra were analysed using Athena and Artemis from the Demeter IFEFFIT package [25,26].

2.3. Catalytic tests

2.3.1. Cinnamyl alcohol oxidation

The reactions were carried out in a thermostat controlled stainless steel reactor (30 mL) agitated with an electronically controlled magnetic stirrer connected to a large reservoir (5000 mL) containing oxygen at 2 atm. The oxygen uptake was followed by a mass flow controller connected to a PC through an A/D board. The oxidation experiments were carried out in xylene (0.3 M substrate, substrate/Pd = 1000 (mol/mol), 80 °C, pO_2 = 2 atm). The reaction was monitored by analysing periodically withdrawn samples. Mass balances, in the analysis, were always 98% ± 3. Analyses were performed using a HP 7820A gas chromatograph equipped with a capillary column HP-5 30 m × 0.32 mm, 0.25 μm Film, by Agilent Technologies. Authentic samples were analysed to determine separation times. Identification of products was performed using a Thermo Scientific Trace ISQ QD Single Quadrupole GC–MS equipped with a capillary column HP-5 30 m × 0.32 mm, 0.25 μm Film, by Agilent Technologies. Quantitative analyses with external standard

Table 1
Cinnamyl alcohol oxidation.[a]

Catalyst	TOF[b] h^{-1}	Selectivity (at 90% conv)				
		cinnamaldehyde	3-phenyl propanol	3-phenyl propanal	Styrene	Benzaldehyde
Pd/AC	253	69	27	2	2	1
AuPd/AC	402	80	2	11	–	3
AuPdBi/AC	315	94	1	3	–	1
Bi$_2$O$_3$ + AuPd/AC	389	79	5	11	1	3

[a] Reaction conditions: 0.3 M cinnamyl alcohol (in xylene as solvent), Pd/substrate 1/1000 (molar ratio), 80 °C, 2 bar O$_2$.

[b] Calculated as mol of converted reagent per mol of metal (considering all metal species) after 15 min.

method (n-octanol) was used.

2.3.2. Cinnamaldehyde hydrogenation

The reactions were carried out in a thermostatted stainless steel reactor (30 mL) agitated with an electronically controlled magnetic stirrer. The hydrogenation experiments were carried out in xylene (0.3 M substrate, substrate/Pd = 1000 (mol/mol), 25 °C, pH$_2$ = 1 atm). The reaction was monitored by analysing periodically withdrawn samples. Mass balances, in the analysis, were always 98% ± 3. Analyses were performed using a HP 7820A gas chromatograph equipped with a capillary column HP-5 30 m × 0.32 mm, 0.25 μm Film, by Agilent Technologies. Authentic samples were analysed to determine separation times. Identification of products was performed using a Thermo Scientific Trace ISQ QD Single Quadrupole GC–MS equipped with a capillary column HP-5 30 m × 0.32 mm, 0.25 μm Film, by Agilent Technologies. Quantitative analyses with external standard method (n-octanol) was used.

3. Results and discussion

1 wt% AuPd/AC catalyst (Au:Pd molar ratio 6:4) was prepared by an established two step procedure, able to produce alloyed structures as we have shown in previous publications [27,28]. The bimetallic catalyst has been modified by subsequent Bi deposition to prepare a trimetallic AuPdBi/AC catalyst (1 wt% Bi loading).

The bimetallic and trimetallic catalysts were tested in both oxidation and hydrogenation model reactions. The comparison with monometallic Pd/AC catalyst allowed to reveal the synergistic effects deriving from the addition of Au and Bi in bimetallic and trimetallic catalysts, respectively. Cinnamyl alcohol was selected as a model substrate to evaluate the catalytic performances of as prepared materials in liquid phase oxidation processes, using xylene as solvent. The main results are summarized in Table 1.

The oxidation of cinnamyl alcohol on Pd/AC catalyst produced cinnamaldehyde (69% selectivity at 90% conversion) and a large amount of 3-phenylpropanol (27%) as by-product deriving from the hydrogenation of the C═C bond. As reported above, according to the literature the hydrogenation of the double bond is promoted by the formation of Pd─H species during the dehydrogenation process [29].

Although metal hydride species should be expected to react with oxygen to form water or hydrogen peroxide, actually substrate and product molecules can compete with oxygen for these species. The occurrence of hydrogenation and hydrogenolysis reactions even under aerobic conditions has been reported by Keresszegi et al. [30], which observed the formation of products from hydrogenation and hydrogenolysis reaction over Pd/Al$_2$O$_3$ even in the presence of molecular oxygen, which is more likely responsible for oxidative removal of degradation products. In situ XAFS studies by Lee et al. demonstrated that oxygen has an active role in minimizing the adsorbate-induced catalyst reduction and restructuring phenomena on Pd/C catalyst, by restoring surface PdO$_x$ species which are responsible for high activity and selectivity in cinnamyl alcohol oxidation [31]. More recently, Rucinska et al. investigated the role of oxygen in the cinnamyl alcohol oxidation over 1%AuPd/TiO$_2$ catalysts under experimental conditions

Table 2
3-phenyl propanol oxidation.[a]

Catalyst	TOF[b] h^{-1}	Selectivity (at 30% conv)	
		3-phenylpropanal	Benzaldehyde
Pd/AC	10	90	9
AuPd/AC	89	96	4
AuPdBi/AC	75	98	2
Bi$_2$O$_3$ + AuPd/AC	83	95	4

[a] Reaction conditions: 0.3 M 3-phenyl propanol (in xylene as solvent), Pd/substrate 1/1000 (molar ratio), 80 °C, 2 bar O$_2$.

[b] Calculated as mol of converted reagent per mol of metal (considering all metal species) after 15 min.

(solvent: toluene, pO$_2$ = 3 bar and T = 120 °C) close to those used in this work [32]. A higher selectivity to cinnamaldehyde was attained under aerobic conditions compared to unaerobic conditions (3 bar N$_2$), however also in this case hydrogenation/hydrogenolysis products were formed and accounted for ca. 15%, in agreement to the results reported in Table 2.

Alloying Au to Pd resulted in a catalyst 1.5 times more active than monometallic Pd (253 h^{-1} vs. 402 h^{-1} TOF for Pd and AuPd, respectively) and limited the hydrogenation of the C═C bond compared to Pd (27% vs. 2% selectivity to 3-phenylpropanol, and 69% vs. 80% selectivity to cinnamaldehyde on Pd and AuPd, respectively). In addition, the 3-phenylpropanol produced in more modest amount, was further oxidized to the corresponding aldehyde (3-phenylpropanal). These results suggested that *i)* the addition of Au prevented the formation of Pd─H species, as reported in the literature [33,34], thus limiting the hydrogenation of the C═C bond; *ii)* Pd is less prone to oxidize non activated –OH group than AuPd. This evidence was further corroborated by a further experiment consisting in 3-phenyl propanol oxidation (as an intermediate of cinnamyl alcohol oxidation), which confirmed the observed catalytic trend, being Pd about 7.5 times less active (TOF 10 h^{-1}) than AuPd (TOF 75 h^{-1}) in the specific reaction (Table 2).

When trimetallic AuPdBi catalyst was tested in cinnamyl alcohol oxidation, the catalytic activity was increased by a factor of 1.25

Table 3
Cinnamaldehyde hydrogenation.[a]

Catalyst	TOF[b] h^{-1}	Selectivity (at 90% conv)			
		3-Phenyl propanal	3-phenyl propanol	1-phenyl propane	Cinnamyl alcohol
Pd/AC	1274	65	28	1	3
AuPd/AC	1425	70	26	–	2
AuPdBi/AC	1209	93	5	–	2
Bi$_2$O$_3$ + AuPd/AC	1410	72	24	2	2

[a] Reaction conditions: 0.3 M cinnamaldehyde (in xylene as solvent), Pd/substrate 1/1000 (molar ratio), 25 °C, 1 bar H$_2$.

[b] Calculated as mol of converted reagent per mol of metal (considering all metal species) after 15 min.
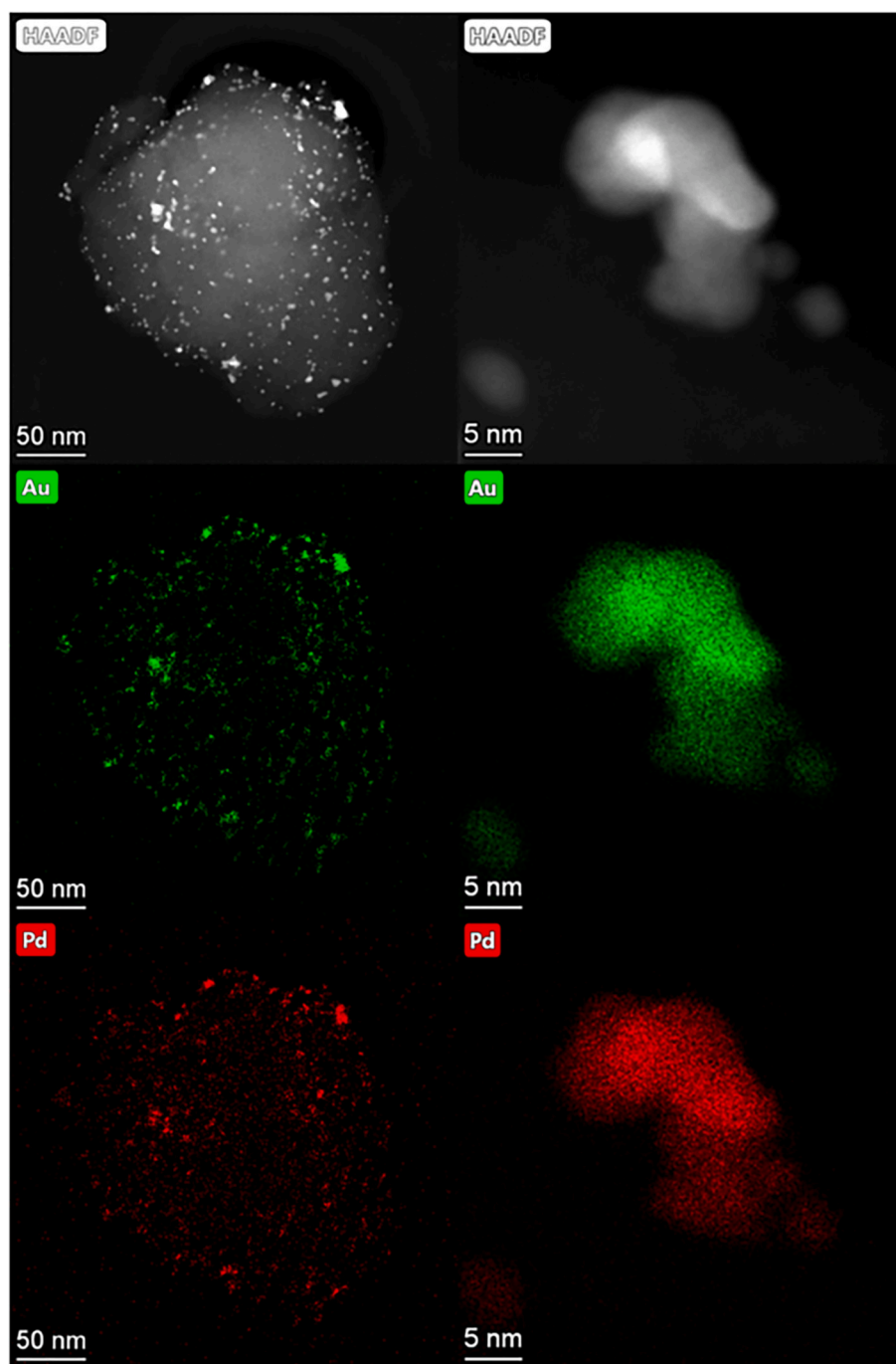
Fig. 1. STEM-EDX analysis of AuPd/AC catalyst particles displaying HAADF images (top), Au intensity maps (middle), and Pd intensity maps (bottom).

compared to Pd catalyst, even if ca. 20% decrease in activity (315 h^{-1}) was observed compared to bimetallic AuPd catalyst (402 h^{-1}). Interestingly, for the trimetallic catalysts, the oxidation of cinnamyl alcohol proceeded with a very high selectivity to cinnamaldehyde (90%). This experimental evidence suggested that Bi significantly suppresses the C═C hydrogenation process in agreement with current literature [14]. Phenylpropanal and phenylpropanol were present just as traces, the former deriving from the oxidation of the latter, as confirmed by 3-phenyl propanol oxidation tests (Table 2).

To better understand the effect of Bi in the hydrogenation activity of catalysts, interesting considerations could be drawn from the evaluation of the catalytic performances in cinnamaldehyde hydrogenation reaction in terms of reduction of the C═C or C═O functional group (Table 3).
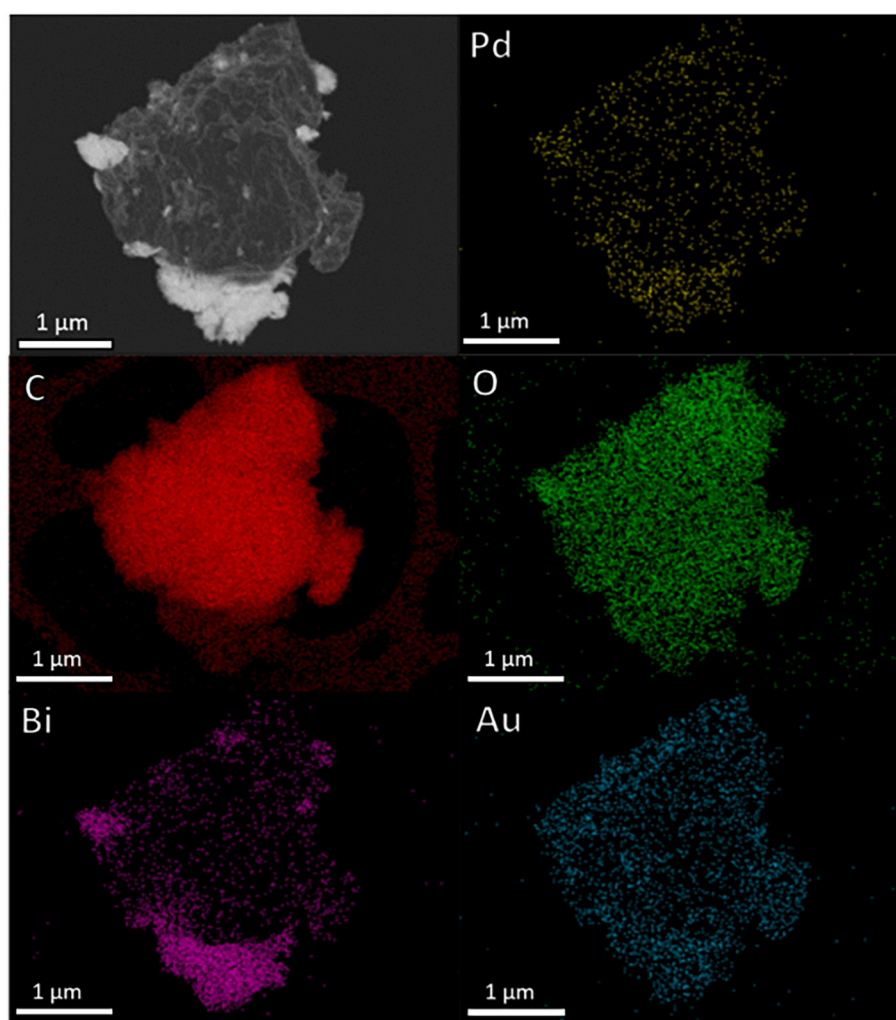
Comparing Pd, AuPd and AuPdBi, in terms of activity the same trend was observed as in the case of the oxidation reaction. Alloying Au to Pd led to a higher catalytic activity by a factor of 1.12 than monometallic Pd (1425 and 1274 h^{-1} for AuPd and Pd respectively) whereas the addition of Bi slightly decreased the activity (1209 h^{-1}). However, the differences in the activity were not as remarkable as in the case of oxidation reaction. More interestingly, concerning the selectivity, the addition of Bi enhanced the selectivity to 3-phenylpropanal (from 70% with AuPd to 93% in the case of AuPdBi), i.e. the C═C hydrogenation product, while it inhibited the formation of 3-phenylpropanol, which was present in discrete amount in the case of Pd and AuPd catalysts and could derive from the further hydrogenation of 3-phenylpropanal or from cinnamyl alcohol hydrogenation pathway.

In order to understand the catalytic role of bismuth in relation with

Table 4

Results of the EXAFS fitting procedure on bimetallic and trimetallic catalysts.

		M-M Bond	N	R / Å	$\Delta\sigma^2$	ΔE	χ^2	R Factor
Au L$_3$ Edge	AuPd/C[a]	Au-Au	7.2(5)	2.815(5)	0.0092(6)	4.1(4)	104	0.004
		Au-Pd	3.1(5)	2.794 (6)	0.0080(7)			
	AuPdBi/C[a]	Au-Au	6.6(7)	2.813(7)	0.0085(7)	3.9(6)	259	0.011
		Au-Pd	3.1(5)	2.789(9)	0.008(1)			
Pd K Edge	AuPd/C[a]	Pd-Pd	2.8(8)	2.78(2)	0.009(2)	−9 (1)	204	0.016
		Pd-Au	8(1)	2.78(1)	0.010(2)			
	AuPdBi/C[b]	Pd-Pd	2.9(7)	2.78(2)	0.008(2)	−8.5(9)	113	0.015
		Pd-Au	7(1)	2.79(1)	0.008(1)			
		Bond	N	R / Å	$\Delta\sigma^2$	ΔE	χ^2	R Factor
Bi L$_2$ Edge	AuPdBi/C[c]	Bi-Bi	5(set)	3.71(2)	0.024(3)	−4.1(5)	20.86	0.004
		Bi-O1	1.3(1)	2.24(3)	0.001(3)			
		Bi-O2	1.5(5)	3.31(2)	0.007(5)			
		Bi-O3.1	1.0(4)	2.12(3)	0.001(3)			
		Bi-O3.2	0.6(2)	2.39(3)	0.001(3)			

[a] Fit Range 3 < k < 14, 1.25 < R < 3, Number of Independent Points 11.
[b] Fit Range 3 < k < 14, 1.2 < R < 3, Number of Independent Points 12.
[c] Fit range 2 < k < 10, 1 < R < 4, Number of Independent Points 15.

Fig. 2. SEM-EDX analysis of AuPdBi/AC catalyst.

its insertion in the preformed AuPd structure, morphological and structural characterization of bimetallic and trimetallic catalysts was performed.

Particle size distributions from TEM analyses (Fig. S1) demonstrated that both monometallic (Pd/AC), bimetallic (AuPd/AC) had similar mean particle sizes (3.2–3.9 nm), as typically observed in catalysts

prepared by this specific sol-immobilisation procedure.

Scanning transmission electron microscopy (STEM) coupled with elemental mapping by energy dispersive X-ray (EDX) spectroscopy confirmed the presence of random-alloyed structure of bimetallic AuPd nanoparticles in AuPd/AC catalyst (Fig. 1).

X-ray absorption spectra (EXAFS) at the Pd K-edge and Au L$_3$-edge

(Fig. S2) and values of coordination numbers (N), nearest-neighbours distances (R) and Debye-Waller factors (σ^2) reported in Table 4 confirmed the formation of an AuPd alloy. Actually, the presence of Au—Pd bonds was clearly observed and Pd—Pd and Au—Au distances were comparable to the Pd—Au (Tables 4). The alloyed structure of AuPd was maintained also in the trimetallic catalysts, while concerning bismuth EXAFS data analysis indicates the presence of only a Bi—O and a Bi—Bi coordination.

It seems, then, that Bi is not alloyed with Au and Pd rather it is present as a segregated bismuth oxide phase. Even if an alloyed structure between Au, Pd and and Bi cannot be supposed on the basis of EXAFS, we might guess that the bismuth oxide phase is in the close proximity of AuPd NPs. In fact, SEM-EDX analysis revealed the co-presence of tri-metallic systems with homogeneous Au, Pd, Bi distribution in close contact with a segregated bismuth phase as is shown in Fig. 2. In any case, the occurrence of moderate segregation did not alter the mean particle size (Fig. S1).

The modification of activity and selectivity observed for trimetallic AuPdBi catalysts could be ascribed to the presence of bismuth oxide phase highly dispersed and in intimate contact with Au and Pd sites. Indeed, when a physical mixture of Bi_2O_3 mixed to the bimetallic AuPd/AC catalyst is tested both for the model oxidation and hydrogenation reactions (Tables 1, 2 and 3, entry 4). No significant differences in activity and selectivity were observed compared to AuPd/AC, thus suggesting that when introduced as physical mixture bismuth oxide acts as spectator species.

We propose that the deposition of highly dispersed bismuth phase provokes a partial blockage of a fraction of active sites, which could be likely responsible for both selectivity enhancement and slight activity drop. However, we cannot exclude that the interaction of bismuth with AuPd might also cause a modification of the electron density on the metal sites (e.g. charge transfer effects).

4. Conclusions

Investigations on trimetallic AuPdBi/AC catalysts revealed that bismuth slightly depresses the activity of AuPd alloyed NPs and modifies the selectivity in both oxidation and hydrogenation reactions in agreement with previous reports. Structural, compositional and morphological characterization revealed the co-presence of segregated bismuth oxide and trimetallic AuPdBi nanoparticles. This outcome suggests that Bi basically acts as a "physical" blocker for the most active sites on AuPd NPs, limiting the occurrence of consecutive reactions. The addition of low amount of bismuth (1 wt%) to AuPd NPs thus appears as a good compromise to achieve a significative enhancement of selectivity with negligible decrease in the activity. Further experimental (e.g. CO chemisorption) and theoretical studies are still needed, aimed to identify the nature of blocked active sites on AuPd NPs (e.g. atoms at corners, edges, low-coordination sites) and their interactions with bismuth phase. The effect of the synthesis conditions, and in particular the role of stabilizing agent (PVA) in controlling the dispersion and sitting of Bi phase, are additional aspects which deserve to be investigated in more detail.

Author statement

Sebastiano Campisi: Conceptualization, Methodology, Writing-Original draft preparation, Writing- Reviewing and Editing, Supervision. Sofia Capelli: Visualisation, Investigation, Validation. Michele Ferri: Visualization, Investigation, Validation. Alberto Villa: Conceptualization, Methodology, Writing- Reviewing and Editing. Ellie Dann: Software, Data Curation, Validation. Austin Wade: Investigation, Data Curation, Visualisation. Peter P. Wells: Conceptualization, Methodology, Writing- Reviewing and Editing, Nikolaos Dimitratos: Conceptualization, Methodology, Writing- Reviewing and Editing, Supervision.

Declaration of Competing Interest

The authors declare that they have no known competing financial interests or personal relationships that could have appeared to influence the work reported in this paper.

Appendix A. Supplementary data

Supplementary data to this article can be found online at https://doi.org/10.1016/j.catcom.2021.106340.

References

[1] T. Ollevier, New trends in bismuth-catalyzed synthetic transformations, Org. Biomol. Chem. 11 (2013) 2740–2755, https://doi.org/10.1039/c3ob26537d.

[2] M. Besson, P. Gallezot, Selective oxidation of alcohols and aldehydes on metal catalysts, Catal. Today 57 (2000) 127–141.

[3] J.H. Wu, F.Q. Shao, X.Q. Luo, H.J. Xu, A.J. Wang, Pd nanocones supported on g-C 3 N 4 : an efficient photocatalyst for boosting catalytic reduction of hexavalent chromium under visible-light irradiation, Appl. Surf. Sci. 471 (2019) 935–942, https://doi.org/10.1016/j.apsusc.2018.12.075.

[4] C. Zhou, Z. Guo, Y. Dai, X. Jia, H. Yu, Y. Yang, Promoting role of bismuth on carbon nanotube supported platinum catalysts in aqueous phase aerobic oxidation of benzyl alcohol, Appl. Catal. B Environ. 181 (2016) 118–126, https://doi.org/10.1016/j.apcatb.2015.07.048.

[5] C.E. Chan-Thaw, A. Villa, G.M. Veith, K. Kailasam, L.A. Adamczyk, R.R. Unocic, L. Prati, A. Thomas, Influence of periodic nitrogen functionality on the selective oxidation of alcohols, Chem. - An Asian J. 7 (2012) 387–393, https://doi.org/10.1002/asia.201100565.

[6] D. Ferri, A. Baiker, Advances in infrared spectroscopy of catalytic solid-liquid interfaces: the case of selective alcohol oxidation, Top. Catal. 52 (2009) 1323–1333, https://doi.org/10.1007/s11244-009-9310-5.

[7] S. Garcia-Segura, J.D. Ocon, M.N. Chong, Electrochemical oxidation remediation of real wastewater effluents — a review, Process. Saf. Environ. Prot. 113 (2018) 48–67, https://doi.org/10.1016/j.psep.2017.09.014.

[8] D. Motta, F.J. Sanchez, N. Dimitratos, A. Villa, L. Prati, An investigation on AuPt and AuPt-Bi on granular carbon as catalysts for the oxidation of glycerol under continuous fl ow conditions, Catal. Today 308 (2018) 50–57, https://doi.org/10.1016/j.cattod.2017.10.012.

[9] M. Wenkin, P. Ruiz, B. Delmon, M. Devillers, The role of bismuth as promoter in Pd-Bi catalysts for the selective oxidation of glucose to gluconate, J. Mol. Catal. A Chem. 180 (2002) 141–159, https://doi.org/10.1016/S1381-1169(01)00421-6.

[10] H. Ait Rass, N. Essayem, M. Besson, Selective aqueous phase oxidation of 5-hydroxymethylfurfural to 2,5-furandicarboxylic acid over Pt/C catalysts: influence of the base and effect of bismuth promotion, Green Chem. 15 (2013) 2240–2251, https://doi.org/10.1039/c3gc40727f.

[11] F. Alardin, H. Wullens, S. Hermans, M. Devillers, Mechanistic and kinetic studies on glyoxal oxidation with bi- and Pb-promoted Pd/C catalysts, J. Mol. Catal. A Chem. 225 (2005) 79–89, https://doi.org/10.1016/j.molcata.2004.08.030.

[12] K. Zhou, W. Wang, Z. Zhao, G. Luo, J.T. Miller, M.S. Wong, F. Wei, Synergistic gold-bismuth catalysis for non-mercury hydrochlorination of acetylene to vinyl chloride monomer, ACS Catal. 4 (2014) 3112–3116, https://doi.org/10.1021/cs500530f.

[13] C. Jeyabharathi, J. Mathiyarasu, K.L.N. Phani, Methanol tolerant oxygen-reduction activity of carbon supported platinum-bismuth bimetallic nanoparticles, J. Appl. Electrochem. 39 (2009) 45–53, https://doi.org/10.1007/s10800-008-9638-8.

[14] N. Cherkasov, A.O. Ibhadon, A.J. McCue, J.A. Anderson, S.K. Johnston, Palladium-bismuth intermetallic and surface-poisoned catalysts for the semi-hydrogenation of 2-methyl-3-butyn-2-ol, Appl. Catal. A Gen. 497 (2015) 22–30, https://doi.org/10.1016/j.apcata.2015.02.038.

[15] X. Ning, Y. Li, B. Dong, H. Wang, H. Yu, F. Peng, Y. Yang, Electron transfer dependent catalysis of Pt on N-doped carbon nanotubes: effects of synthesis method on metal-support interaction, J. Catal. 348 (2017) 100–109, https://doi.org/10.1016/j.jcat.2017.02.011.

[16] M. Simões, S. Baranton, C. Coutanceau, Influence of bismuth on the structure and activity of Pt and Pd nanocatalysts for the direct electrooxidation of NaBH4, Electrochim. Acta 56 (2010) 580–591, https://doi.org/10.1016/j.electacta.2010.09.006.

[17] C. Mondelli, J.D. Grunwaldt, D. Ferri, A. Baiker, Role of Bi promotion and solvent in platinum-catalyzed alcohol oxidation probed by in situ X-ray absorption and ATR-IR spectroscopy, Phys. Chem. Chem. Phys. 12 (2010) 5307–5316, https://doi.org/10.1039/b926833b.

[18] K. Roy, L. Artiglia, Y. Xiao, A. Varma, J.A. Van Bokhoven, Role of bismuth in the stability of Pt–Bi bimetallic catalyst for methane mediated deoxygenation of guaiacol, an APXPS study, ACS Catal. 9 (2019) 3694–3699, https://doi.org/10.1021/acscatal.8b04699.

[19] W. Hu, B. Lowry, A. Varma, Kinetic study of glycerol oxidation network over Pt-Bi/C catalyst, Appl. Catal. B Environ. 106 (2011) 123–132, https://doi.org/10.1016/j.apcatb.2011.05.015.

[20] I.A. Witońska, M.J. Walock, P. Dziugan, S. Karski, A.V. Stanishevsky, The structure of Pd-M supported catalysts used in the hydrogen transfer reactions (M = In, Bi and Te), Appl. Surf. Sci. 273 (2013) 330–342, https://doi.org/10.1016/j.apsusc.2013.02.039.

[21] A.S. Bauskar, C.A. Rice, Spontaneously Bi decorated carbon supported Pd nanoparticles for formic acid electro-oxidation, Electrochim. Acta 107 (2013) 562–568, https://doi.org/10.1016/j.electacta.2013.06.042.

[22] A. Villa, D. Wang, G.M. Veith, L. Prati, Bismuth as a modifier of Au – Pd catalyst : enhancing selectivity in alcohol oxidation by suppressing parallel reaction, J. Catal. 292 (2012) 73–80, https://doi.org/10.1016/j.jcat.2012.04.021.

[23] C.E. Chan-Thaw, A. Villa, D. Wang, V.D. Santo, A. Orbelli Biroli, G.M. Veith, A. Thomas, L. Prati, PdHx entrapped in a covalent triazine framework modulates selectivity in glycerol oxidation, ChemCatChem. 7 (2015) 2149–2154, https://doi.org/10.1002/cctc.201500055.

[24] A. Savara, C.E. Chan-Thaw, I. Rossetti, A. Villa, L. Prati, Benzyl alcohol oxidation on carbon-supported Pd nanoparticles: elucidating the reaction mechanism, ChemCatChem. 6 (2014) 3464–3473, https://doi.org/10.1002/cctc.201402552.

[25] B. Ravel, M. Newville, ATHENA, ARTEMIS, HEPHAESTUS: data analysis for X-ray absorption spectroscopy using IFEFFIT, J. Synchrotron Radiat. 12 (2005) 537–541, https://doi.org/10.1107/S0909049505012719.

[26] M. Newville, IFEFFIT: interactive XAFS analysis and FEFF fitting, J. Synchrotron Radiat. 8 (2001) 322–324, https://doi.org/10.1107/S0909049500016964.

[27] A. Villa, D. Wang, D. Su, G.M. Veith, L. Prati, Using supported au nanoparticles as starting material for preparing uniform Au/Pd bimetallic catalysts, Phys. Chem. Chem. Phys. 12 (2010) 2183–2189, https://doi.org/10.1039/b919322g.

[28] D. Wang, A. Villa, F. Porta, D. Su, L. Prati, Single-phase bimetallic system for the selective oxidation of glycerol to glycerate, Chem. Commun. (2006) 1956–1958, https://doi.org/10.1039/b518069d.

[29] A. Villa, N. Janjic, P. Spontoni, D. Wang, D.S. Su, L. Prati, Au-Pd/AC as catalysts for alcohol oxidation: effect of reaction parameters on catalytic activity and selectivity, Appl. Catal. A Gen. 364 (2009) 221–228, https://doi.org/10.1016/j.apcata.2009.05.059.

[30] C. Keresszegi, T. Burgi, T. Mallat, A. Baiker, On the role of oxygen in the liquid-phase aerobic oxidation of alcohols on palladium, J. Catal. 211 (2002) 244–251, https://doi.org/10.1006/jcat.2002.3723.

[31] A.F. Lee, K. Wilson, Structure–reactivity correlations in the selective aerobic oxidation of cinnamyl alcohol: in situ XAFS, Green Chem. 6 (2004) 37–42, https://doi.org/10.1039/b310505a.

[32] E. Rucinska, P.J. Miedziak, S. Pattisson, G.L. Brett, S. Iqbal, D.J. Morgan, M. Sankar, G.J. Hutchings, Cinnamyl alcohol oxidation using supported bimetallic Au-Pd nanoparticles: an investigation of autoxidation and catalysis, Catal. Sci. Technol. 8 (2018) 2987–2997, https://doi.org/10.1039/c8cy00155c.

[33] S. Luo, D. Wang, T.B. Flanagan, Thermodynamics of hydrogen in fcc Pd-Au alloys, J. Phys. Chem. B 114 (2010) 6117–6125, https://doi.org/10.1021/jp100858r.

[34] K. Sun, A.R. Wilson, S.T. Thompson, H.H. Lamb, Catalytic deoxygenation of octanoic acid over supported palladium: effects of particle size and alloying with gold, ACS Catal. 5 (2015) 1939–1948, https://doi.org/10.1021/cs501865n.